Thermoelectric power in alloys with phase separation (composites)

2009 J. Phys.: Condens. Matter 21 175703

(http://iopscience.iop.org/0953-8984/21/17/175703)

IOP PUBLISHING JOURNAL OF PHYSICS: CONDENSED MATTER

J. Phys.: Condens. Matter **21** (2009) 175703 (8pp) doi:10.1088/0953-8984/21/17/175703

Thermoelectric power in alloys with phase separation (composites)

Joachim Sonntag

MEAS Deutschland GmbH-HL-Planartechnik, Hauert 13, D-44227 Dortmund, Germany

E-mail: joachim.sonntag@meas-spec.com

Received 9 December 2008, in final form 6 March 2009
Published 30 March 2009
Online at stacks.iop.org/JPhysCM/21/175703

Abstract

A thermopower formula is derived for composites: $\sum_i \upsilon_i \frac{\kappa_i/S_i-\kappa/S}{\kappa_i/S_i+2\kappa/S} = 0$ (κ_i and κ are the specific thermal conductivities, S_i and S are the Seebeck coefficients of the phase i and the composite, respectively, and υ_i is the volume fraction of the phase i). This formula can be applied for calculating the Seebeck coefficient (thermoelectric power) of amorphous transition-metal–metalloid alloys, for which amorphous phase separation occurs for large ranges of concentration. There are two contributions to S_i, a scattering term and a contribution due to electron transfer between the phases maintaining a common electrochemical potential μ. The theory predicts discontinuities in the concentration dependence of the Seebeck coefficient of metallic composites. It is argued that in amorphous composites these discontinuities occur very precisely at $\upsilon_i = 1/3$. This phenomenon can be used to characterize the crystallization kinetics of amorphous alloys. The theory is applied to a-$\text{Cr}_{1-x}\text{Si}_x$ alloys for calculation of S versus x. Both the calculated $S(x)$ dependence and the discontinuities agree very well with the experimental data, as long as $x < 0.67$; the deviations at $x > 0.67$ are interpreted to be caused by the p–d bonds at the phase boundaries.

1. Introduction

In a previous paper [1] a thermopower formula has been derived for alloys with phase separation (composites). This thermopower formula (equation (30), respectively equation (32), in [1]) is an approximation formula, which in addition holds only for the special case of composites with metallic phases.

The purpose of the present paper is the derivation of a thermopower formula for composites for the general case, where the phases can be metallic and/or semiconducting ones[1]. This derivation will be based on J and J_S, the electric and entropy-flux density, respectively, while the derivation in [1] was based on J and J_Q. J_Q is the heat current density. For the one-band models, it makes little difference whether one chooses to interpret thermoelectric phenomena on the basis of J and J_Q, or J and J_S. However, for two-band or multiband models characteristic for semiconductors, the use of J and J_Q leads to complications, which are not to be expected if J and J_S are used as a basis (Harman and Honig [2], p 28).

For the derivation the following assumptions are made: (a) elastic scattering, (b) $\upsilon_i > 1/3$ for each phase i and (c) the phase grains are spherical without preferred orientations and arranged in a symmetrical fashion. υ_i is the volume fraction of the phase i. Assumptions (a) and (b) allow the application of the relaxation time approximation of the Boltzmann transport equation (BTE) to each phase of a composite, and assumption (c) allows the application of the effective medium theory (EMT).

Starting with the local electric and entropy-flux density for a single phase i, J_i and $J_{S,i}$, respectively, and applying EMT, in section 2 the thermopower formula for composites will be derived. In section 3 a guide is proposed for a practical calculation of the transport coefficients of the phases required for a calculation of the Seebeck coefficient of a composite, and the influence of the electrochemical potential on the Seebeck coefficient will be considered. In section 4 the theory will be applied for the calculation of the Seebeck coefficient versus x for a-$\text{Cr}_{1-x}\text{Si}_x$ alloys and compared with experimental data as well as with earlier calculations. In section 5.1 the derived thermopower formula for composites

---

[1] In the scientific literature there also exist other thermopower formulae for composites [36–48]. These formulae are different from the ones derived in [1] and in the present paper, because there the influence of the electrochemical potential and its change with temperature and concentration is generally not considered.

will be compared with the thermopower formula derived in [1] and the conditions for applicability are defined. In section 5.2 the calculation of the transport coefficients of the phases will be considered for the case that assumption (b), $\upsilon_i > 1/3$, is not fulfilled; the consequences of this discussion can be used for a characterization of the crystallization kinetics of amorphous alloys, as will be discussed in section 5.3. In section 6 the results will be summarized.

2. Thermopower formula for composites

J_i and $J_{S,i}$ can be written [2, 3]

$$J_i = \sigma_i[\text{grad}(\mu_i/|e|) - S_i\text{grad}T], \tag{1}$$

$$J_{S,i} = \sigma_i S_i \text{grad}(\mu_i/|e|) - (\sigma_i S_i^2 + \kappa_i/T)\text{grad}T, \tag{2}$$

where T and $|e|$ are the temperature and the elementary charge, respectively. σ_i, κ_i, S_i and μ_i are the specific electrical conductivity, specific thermal conductivity, Seebeck coefficient[2] and electrochemical potential, respectively, in the phase i.

According to the strategy underlying the EMT, we demand continuity of the entropy-flux density and the electrochemical potential and their gradients at the boundary face between a single phase grain and its surrounding (effective medium), where additionally $J = J_i = 0$ is to be fulfilled. Setting $J_i = 0$ in equation (1), and inserting into equation (2), one obtains for the local entropy-flux density:

$$J_{S,i} = -\frac{\kappa_i}{S_i T}\text{grad}(\mu_i/|e|). \tag{3}$$

In analogy to equation (3) we write for the total entropy-flux density J_S in the specimen

$$J_S = -\frac{\kappa}{ST}\text{grad}(\mu/|e|), \tag{4}$$

where κ, S and μ are the specific thermal conductivity, the Seebeck coefficient and the electrochemical potential, respectively, of the composite (see footnote 2).

Equations (3) and (4) have the same structure as equations (18) and (20) of [1]; that is why we can apply the same formalism as described in [1] (equations (23)–(30), (A1)–(A8) therein), however, with other starting equations

$$J_S = \langle J_{S,i}\rangle, \tag{5}$$

$$\text{grad}\mu = \langle \text{grad}\mu_i\rangle, \tag{6}$$

where the angular brackets characterize the averages. Equations (5) and (6) replace equations (23) and (24) of [1] and μ (respectively μ_i) takes the role of the potential. Applying this formalism to equations (5) and (6), one obtains

$$\sum_i \upsilon_i \frac{\kappa_i/S_i - \kappa/S}{\kappa_i/S_i + 2\kappa/S} = 0. \tag{7}$$

Equation (7) completes the set of the fundamental formulae for the transport coefficients of composites which are

$$\sum_i \upsilon_i \frac{\kappa_i - \kappa}{\kappa_i + 2\kappa} = 0, \tag{8}$$

$$\sum_i \upsilon_i \frac{\sigma_i - \sigma}{\sigma_i + 2\sigma} = 0, \tag{9}$$

$$\sum_i \upsilon_i \frac{\sigma_i^2 R_{\text{H},i} - \sigma^2 R_\text{H}}{(\sigma_i + 2\sigma)^2} = 0, \tag{10}$$

derived by Odelevskii [4], Landauer [5], and Cohen and Jortner [6]. σ and R_H are the specific electrical conductivity and the Hall coefficient of the composite, respectively. $R_{\text{H},i}$ is the Hall coefficient of the phase i.

3. Calculation of S_i and κ_i

For calculation of the Seebeck coefficient S of a composite by equation (7), the S_i, κ_i and υ_i as well as κ must be known.

For the Seebeck coefficient of the phase i, the transport theory (BTE) provides for one-band models [2, 3, 7]

$$S_i^0 = \frac{K_{2,i}/K_{1,i} - \mu_i^0}{e_i T}, \tag{11}$$

where the $K_{s,i}$ in equation (11) are the transport integrals:

$$K_{s,i} = -\frac{4}{3m_i}\int E^s \tau_i \frac{\partial f_i(E,T)}{\partial E} N_i(E)\,\text{d}E. \tag{12}$$

$f_i(E, T)$ is the Fermi–Dirac distribution function:

$$f_i(E,T) = \frac{1}{1 + \text{e}^{\frac{E-\mu_i}{k_\text{B}T}}}. \tag{13}$$

E and k_B are the energy and the Boltzmann constant, respectively. $N_i(E)$, m_i, τ_i and μ_i^0 are the density of states, the effective mass, the relaxation time and the chemical potential, respectively, of the carriers in the phase i. $e_i = +|e|$ if the carriers are holes and $e_i = -|e|$ if they are electrons.

The index '0' in S_i^0 characterizes that equation (11) holds for constant carrier density. S_i^0 is identical to α_i as used in [1]. The carrier densities in the phases of a composite are, however, not constant, because there is an electron transfer between the phases to maintain a common electrochemical potential in the composite, i.e.

$$\mu = \mu_i. \tag{14}$$

The temperature-dependent part of this electron transfer between the phases leads to a change of μ, $\text{d}\mu/\text{d}T$, which provides an additional contribution to the thermoelectric power in the phase i:

$$\Delta S = \frac{1}{|e|}\frac{\text{d}\mu}{\text{d}T}, \tag{15}$$

in correspondence with the general definition of the Seebeck coefficient, from the viewpoint of thermodynamics [2, 3]:

$$S = \left[\frac{\text{grad}\mu}{|e|\text{grad}T}\right]_{J=0}. \tag{16}$$

---

[2] The symbols for the Seebeck coefficient (S_i and S) differ from those chosen in [1] (α_i and α), which permitted a direct comparison of the results.

The Seebeck coefficient of the phase i is composed of the scattering term, S_i^0, and the additional term ΔS due to the temperature-dependent part of the electron transfer:

$$S_i = S_i^0 + \Delta S = S_i^0 + \frac{1}{|e|}\frac{\mathrm{d}\mu}{\mathrm{d}T}. \qquad (17)$$

(For a practical calculation of $\mathrm{d}\mu/\mathrm{d}T$ see section III of [1].)

κ can be calculated by equation (8). Assuming that interactions between the various modes of heat transport can be neglected

$$\kappa_i = \kappa_{\mathrm{e},i} + \kappa_{\mathrm{ne},i}, \qquad (18)$$

where $\kappa_{\mathrm{ne},i}$ is the non-electronic contribution to κ_i and $\kappa_{\mathrm{e},i}$ is the electronic contribution. For $\kappa_{\mathrm{e},i}$, the transport theory (BTE) provides for one-band models [2, 3, 7]

$$\kappa_{\mathrm{e},i} = \frac{K_{3,i} - K_{2,i}^2/K_{1,i}}{T}. \qquad (19)$$

For metallic phases, $\kappa_{\mathrm{ne},i}$ can be neglected compared to $\kappa_{\mathrm{e},i}$, if the carrier densities are not too small. Otherwise, the $\kappa_{\mathrm{ne},i}$ are to be determined separately; this becomes especially important for semiconducting phases and if the phase i does not form a macroscopic cluster.

For composites with semiconducting phases, the S_i^0 and $\kappa_{\mathrm{e},i}$ are to be calculated according to the rules for semiconducting solids, in correspondence with the two-band (or multiband) model (see, e.g., Harman and Honig [2], pp 37 and 129), where additionally the condition equation (14) is to be taken into account.

Both the BTE and the approximation of free electrons (NFE approximation) are good descriptions for the phases of amorphous transition-metal–metalloid alloys, as long as $\upsilon_i > 1/3$. This point of view is justified in section IVB of [8]. For metallic phases, equations (11) and (19) are in the NFE approximation [2, 3, 7]

$$S_i^0 = \frac{\pi^2 k_\mathrm{B}^2 T(1 + r_i)}{3e_i E_{\mathrm{F},i}}, \qquad (20)$$

$$\kappa_{\mathrm{e},i} = \frac{16\pi^3}{9}\frac{m_i L_i E_{\mathrm{F},i}}{h^3} k_\mathrm{B}^2 T, \qquad (21)$$

where $E_{\mathrm{F},i}$ is the Fermi energy in the phase i. h is Planck's constant. r_i characterizes the scattering mechanism and represents the energy dependence of the mean free path L_i in the phase i, according to $L_i \propto E^{r_i}$.

The volume fractions of the phases, υ_i, can be calculated from the atomic concentrations of the composite and the phases, x and x_i, respectively. For a two-phase composite, the υ_i can be determined by

$$\upsilon_A = 1 - \upsilon_B = \left[1 + \frac{\mathcal{N}_A(x - x_A)}{\mathcal{N}_B(x_B - x)}\right]^{-1}, \qquad (22)$$

where $\mathcal{N}_A$ and $\mathcal{N}_B$ are the atomic densities in the phases A and B, respectively.

When S_i, κ_i, υ_i and κ are determined, S can be calculated by equation (7). For a two-phase composite, equation (7) has two solutions, $S(-)$ and $S(+)$, in analogy to $\alpha(-)$ and $\alpha(+)$ applied for the two solutions of the approximation formula derived in [1] (equation (35) therein).

4. Calculation of the Seebeck coefficient of a-Cr$_{1-x}$Si$_x$ alloys

Amorphous transition-metal–metalloid alloys are, for large ranges of concentration, composed of different amorphous phases [12–24], each with its own short-range order, a phenomenon called amorphous phase separation. Based on the two-phase model [8] with the two phases a-Cr$_{1-x_A}$Si$_{x_A}$ ($\equiv$phase$A$) and a-Cr$_{1-x_B}$Si$_{x_B}$ ($\equiv$phase$B$), in [1] the Seebeck coefficient of a-Cr$_{1-x}$Si$_x$ has been calculated with the approximation formula of [1] (equation (32) therein). These calculations we have done once more, however with the new thermopower formula, equation (7). The concentration dependences of the calculated values of n, p, L_i, σ_i, S_i^0 ($=\alpha_i$) and σ, are the same as drawn in figures 4(a)–(e) of [1], where n and p is the electron density and hole density in the phases A ($=$a-Cr$_{0.75}$Si$_{0.25}$) and B ($=$a-Cr$_{0.10}$Si$_{0.90}$), respectively, and L_i is the mean free path of the carriers in the phase i. However, c, the parameter characterizing the electrostatic contribution to $\mathrm{d}\mu/\mathrm{d}T$ (section IVA of [1]), is different: $c = 4.85$ eV. c is fitted in such a way that the discontinuity (step) in the calculated $S(-)$ versus x curve coincides with the discontinuity in the experimental data occurring at $x = 0.49$. By change of c only the discontinuity is shifted along the x axis, whereas the shape of the $S(-)$ versus x curve is almost independent of c. This situation is the same as demonstrated in [1] (figure 4(g) therein). As argued in [1], this discontinuity occurs only if the composite is composed of phases with different kinds of carriers, electrons and holes.

In figure 1 the solutions $S(-)$ of equation (7) are drawn versus x, where $\kappa_{\mathrm{ne},i}$ is taken as a parameter. For a-Cr$_{0.10}$Si$_{0.90}$ (the phase B in a-Cr$_{1-x}$Si$_x$), $\kappa_{\mathrm{ne},B}$ is assumed to be equal to $\kappa_{a-\mathrm{Si}}$, the specific thermal conductivity in the amorphous semiconductor a-Si. According to experimental results by Goldsmid *et al* [25], $\kappa_{\mathrm{a-Si}} = 26$ mW cm^{-1} K^{-1}, which corresponds with experimental results by other authors [26–28] at $T = 300$ K.

For a-Cr$_{0.75}$Si$_{0.25}$ (the phase A in a-Cr$_{1-x}$Si$_x$), experimental data for the thermal conductivity, κ_A, are not available and its non-electronic contribution, $\kappa_{\mathrm{ne},A}$, cannot be measured directly because of the simultaneous presence of the relatively large electronic contribution, $\kappa_{\mathrm{e},A}$. That is why we have calculated $S(-)$ for several values of $\kappa_{\mathrm{ne},A}$: $\kappa_{\mathrm{ne},A} = 26$, 13 and 6 mW cm^{-1} K^{-1}. The $S(-)$ curve for $\kappa_{\mathrm{ne},A} = \kappa_{\mathrm{ne},B} = 26$ mW cm^{-1} K^{-1} (not drawn in figure 1) is very similar to those for $\kappa_{\mathrm{ne},A} = \kappa_{\mathrm{ne},B} = 0$.

The value $x_B = 0.90$ applied for the calculations until now is very uncertain. Therefore, the calculations have been done once more, but for $x_B = 1.00$; this value corresponds to the silicon-richest phase in c-Cr$_{1-x}$Si$_x$ (the solubility of Cr atoms in c-Si is very small [29, 30]). The result of these calculations is shown in figure 2. The discontinuity in the calculated

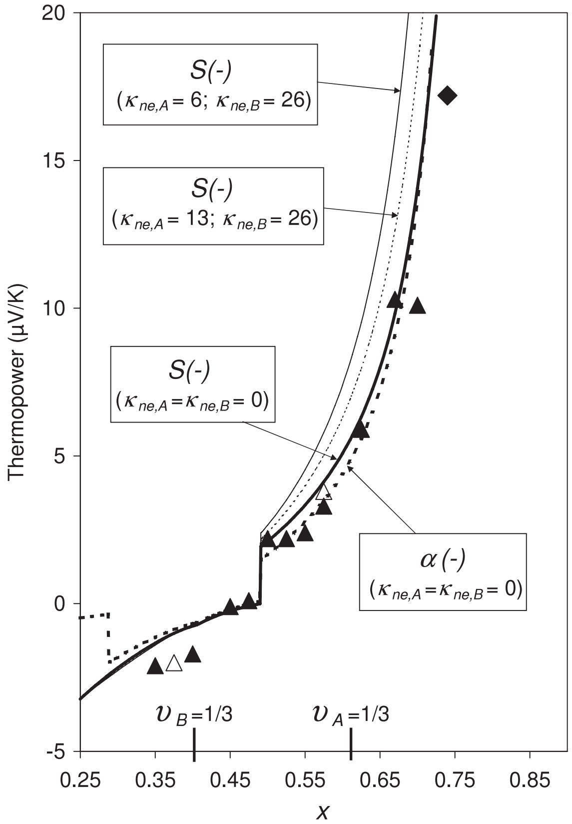

Figure 1. Seebeck coefficient $S(-)$ versus x for a-$\mathrm{Cr}_{1-x}\mathrm{Si}_x$ at $T = 300$ K calculated by equation (7) with $x_A = 0.25$ and $x_B = 0.90$. $\kappa_{\mathrm{ne},i}$ is taken as a parameter as indicated on the curves (in units of mW cm^{-1} K^{-1}). $\alpha(-)$ is the Seebeck coefficient calculated by the approximation formula of [1] (figure 5 therein). The experimental data are taken from Gladun *et al* [9] (diamond), Weser [10] (open triangles) and Sonntag [11][3] (full triangles).

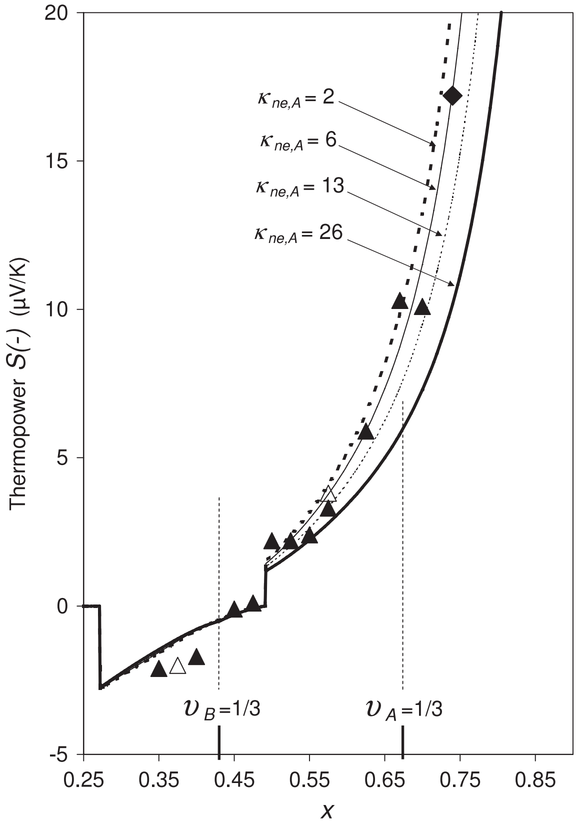

Figure 2. Same as figure 1, however, for $x_B = 1.00$ and $\kappa_{\mathrm{ne},B} = 26$ mW cm^{-1} K^{-1} (for all the curves). 26 mW cm^{-1} K^{-1} is the experimental heat conductivity of amorphous silicon, a-Si [25–28]. $\kappa_{\mathrm{ne},A}$ is taken as a parameter as indicated on the curves (in units of mW cm^{-1} K^{-1}). ($\alpha(-)$ and $S(-)$ for $\kappa_{\mathrm{ne},A} = \kappa_{\mathrm{ne},B} = 0$ are not drawn.)

$S(-)$ curve occurs also at $x = 0.49$, if $c = 2.6$ eV is chosen, determined in the same manner as described earlier.

At present, the values of x_B and $\kappa_{\mathrm{ne},A}$ in a-$\mathrm{Cr}_{1-x}\mathrm{Si}_x$ are very uncertain or not known. Also it could be very useful to measure x_B and κ_A experimentally. A possible way for measuring x_B will be discussed in section 5.3. The knowledge of x_B and $\kappa_{\mathrm{ne},A}$ is especially important for the silicon-rich side, while on the chromium-rich side (to the left of the discontinuity at $x = 0.49$), the different $S(-)$ curves are almost identical; they almost do not depend on x_B and $\kappa_{\mathrm{ne},A}$, as can be seen in figures 1 and 2.

5. Discussion

5.1. Comparison with the thermopower formula of [1]

The essential difference between equation (7) and the thermopower formula derived in [1] (equation (30), respectively equation (32) therein) is the fact that in the former the common electrochemical potential μ occurs (via the S_i, equation (17)), while in the latter one it is the chemical potential of the phases, μ_i^0. This difference is caused by the different basis applied for the derivation of the thermopower formula, namely J and J_Q in [1], but J and J_S in the present paper. After Harman and Honig [2], for the one-band models, it makes little difference whether one chooses to interpret thermoelectric phenomena on the basis of J and J_Q, or J and J_S. However, the use of J and J_Q in two-band or multiband solids leads to severe complications, which are not to be expected if J and J_S are applied as a basis ([2], p 28). That is why equation (7) is to be considered as the thermopower formula which reflects correctly the physical situation, also for composites with two-band or multiband phases.

Although in composites with only metallic phases, each of the phases can be considered as one-band 'solids' (phases), complications arise already in these kinds of composites, because the average $\langle \mathrm{d}\mu_i^0/\mathrm{d}T\rangle$ (equation (22) in [1]) is chosen arbitrarily, which is to be considered as an approximation of the real physical situation. That is why the thermopower formula of [1] is to be considered as an approximation formula for composites with metallic phases (one-band phases). For composites with two-band or multiband phases (e.g. semiconducting phases), the thermopower formula of [1] cannot at all be applied, because it leads to insurmountable difficulties.

The curve $\alpha(-)$ in figure 1 (dotted bold line) calculated with the thermopower formula of [1] (equation (32) therein)

---

[3] The experimental data are cited in [10] (Abb.3 therein).

can be compared directly with $S(-)$ for $\kappa_{\mathrm{ne},i} = 0$ (bold line). This comparison is allowed, because the BTE formulae for $\kappa_{\mathrm{e},i}$ and σ_i are directly proportional to each other, i.e. the result $S(-)$ is not changed, when in equations (7) and (8), κ_i and κ are replaced by σ_i and σ, respectively, provided that $\kappa_{\mathrm{ne},i} = 0$ (in correspondence with the Wiedemann–Franz rule). As can be seen in figure 1, these two curves are similar but not identical; the $\alpha(-)$ curve in figure 1 is to be considered as an approximation of the correct solution $S(-)$ (for $\kappa_{\mathrm{ne},i} = 0$).

Because in equation (7) only transport coefficients and the volume fractions occur, this thermopower formula holds generally, provided that assumption (c) (section 1) is fulfilled and that each of the phases can be characterized by its own specific transport coefficients, κ_i and S_i. Assumptions (a) and (b) must not be fulfilled for equation (7).

5.2. *The transport coefficients of the phases*

The equations for the transport coefficients of the phases, equations (20) and (21), hold only if in the phase i there is a quasi-continuous energy band and that the scattering is elastic, i.e. assumptions (a) and (b) (section 1) must be fulfilled. An equivalent demand according to assumption (b) is the fact that the phase i forms a macroscopic cluster through the composite. With decreasing υ_i, the macroscopic i phase cluster decomposes into separate phase grains; for amorphous composites, this transition occurs very precisely at $\upsilon_i = 1/3$. The reasons are the following.

(1) As the grain diameters are very small (of the order of ~1–2 nm [14, 16]), the number of grains (of the same sort i) must be very large to form a cluster for which a quasi-continuous energy band is realized. Accidentally formed agglomerates of some (for instance, 10 or 100 or 1000) neighbouring grains (with ~1–2 nm diameter) are not sufficient for forming a quasi-continuous energy band.

(2) During the film deposition of a composite, the atoms of the different atom sorts arrive at the substrate equally distributed; therefore the different phase grains (A and B) can also be assumed to be locally equally distributed in the amorphous composite, because the diffusion paths during solidification are very short, which is a prerequisite for forming an amorphous composite.

A phase is an 'electronic phase' determined by a solution of the Schrödinger equation; after hitting the substrate, the atoms move locally only so long until they can form a phase which corresponds to a solution of the Schrödinger equation. That is why the phase grains of the same sort i are also locally equally distributed, as the compositions of the different phases are very different, i.e. the local distribution of the i phase grains is not completely random, as, for example, assumed within the framework of classical percolation theory. For such a locally equally distributed arrangement of the i phase grains in an amorphous matrix (formed by the rest of the composite), it follows that this merging into a macroscopic cluster through the sample occurs very precisely at a specific concentration υ_i; and this specific concentration is $\upsilon_i = 1/3$, as follows, for instance, from equation (9), setting $\sigma_j = 0$ but $\sigma_i \neq 0$ ($j \neq i$). (For a comparison with classical percolation theory concerning this critical value of υ_i, see also [8], section IVA therein.)

(3) A macroscopic i phase cluster is only realized, if all the atoms in this i phase cluster are directly connected to atoms belonging to the same phase sort i. When, for instance, two grains of the same phase sort i are separated by a monoatomic layer of a different(!) phase (j), these two i phase grains cannot be considered as (nearly) one i phase cluster, because the overlap of the electron wavefunctions is interrupted by this monoatomic layer. Within an i phase grain or i phase cluster the wavefunctions, $\psi_i(\mathbf{r})$, overlap, but they do not overlap between two i phase grains or i phase clusters separated by a monoatomic layer of a different(!) phase (j). If a sufficiently large number of i phase grains form a macroscopic cluster, the overlapping wavefunctions $\psi_i(\mathbf{r})$ form a quasi-continuous energy band, while the wavefunctions fall off exponentially in a very short distance $|\delta\mathbf{r}|$ outside this macroscopic cluster. This 'falling off' is comparable with the decrease of the molecular orbitals of (large) molecules at their molecular boundaries (see, e.g., [31], pp 409 and 435, or [32]). Because of this 'non-overlapping' of the $\psi_i(\mathbf{r})$ belonging to different phases, they do not 'penetrate' each other, i.e. there are sharp boundaries between the different (electronic) phases.

Considering the fact that the phase i does not form a quasi-continuous energy spectrum if $\upsilon_i < 1/3$, but a discrete energy spectrum typical for separate grains, then there are no unoccupied states immediately above and below μ (within the energy range $k_{\mathrm{B}}T$), i.e. the electrons cannot be activated to higher energies (at the hot end of the sample) and deliver energy (at the colder end) if $\upsilon_i < 1/3$. Under this condition it follows that $\kappa_{\mathrm{e},i} = 0$ for $\upsilon_i < 1/3$. For S_i the situation is analogous: for $\upsilon_i < 1/3$, $S_i^0 = 0$, i.e. at the transition from $\upsilon_i > 1/3$ to $\upsilon_i < 1/3$ both κ_i and S_i change discontinuously. Such discontinuities are especially to be expected in composites with metallic phases.

For a-Cr$_{1-x}$Si$_x$, $\upsilon_B = 1/3$ and $\upsilon_A = 1/3$ are realized at $x_{\upsilon_B=1/3} = 0.43$ and $x_{\upsilon_A=1/3} = 0.67$, respectively, calculated by equation (22), with $x_A = 0.25$, $x_B = 1.00$, $\mathcal{N}_A = 7.9 \times 10^{22}\ \mathrm{cm}^{-3}$ and $\mathcal{N}_B = 5.0 \times 10^{22}\ \mathrm{cm}^{-3}$. The atomic densities $\mathcal{N}_A$ and $\mathcal{N}_B$ are taken from the crystalline phases, c-Cr$_3$Si [33] and c-Si [34], which are assumed to be approximately equal to the values of the corresponding amorphous phases.

Now we have done the calculations in figure 2 (section 4) once more, but with the difference that $\kappa_{\mathrm{e},i} = S_i^0 = 0$ is set for $x < 0.43$ (corresponding to $\upsilon_B < 1/3$) and for $x > 0.67$ (corresponding to $\upsilon_A < 1/3$); the calculation of $\mathrm{d}\mu/\mathrm{d}T$ is not changed, because the Fermi–Dirac statistics holds for $\upsilon_i < 1/3$ as well. The result is shown in figure 3. At $x = 0.43$ and $x = 0.67$ (corresponding to $\upsilon_B = 1/3$ and $\upsilon_A = 1/3$, respectively) there are really discontinuities in the experimental data. For small x there is an excellent agreement between the experimental data and the calculated ones; the calculated height of the step (discontinuity) at $\upsilon_B = 1/3$ agrees with the experimental data. On the other side, the step

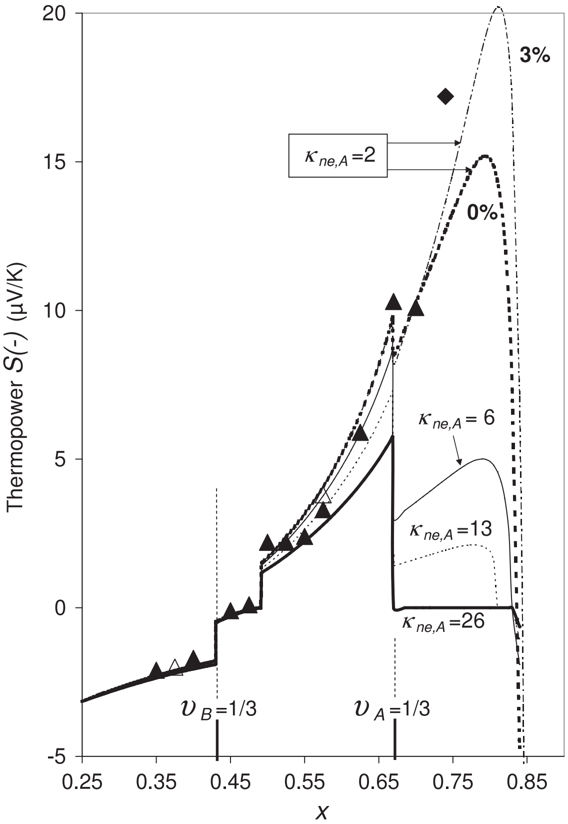

Figure 3. The same as figure 2, where, however, for $x < 0.43$ (corresponding to $\upsilon_B < 1/3$) and $x > 0.67$ (corresponding to $\upsilon_A < 1/3$), $S_i^0 = 0$ and $\kappa_{e,i} = 0$ is set or S_i^0 and $\kappa_{e,i}$ are replaced by $0.03 \times S_i^0$ and $0.03 \times \kappa_{e,i}$ calculated by equation (20) and equation (21), respectively. The latter one is indicated by 3% at the $S(-)$ curve and the former by 0%. For details see section 5.2.

(discontinuity) at $\upsilon_A = 1/3$ corresponds approximately to the experimental data if $\kappa_{ne,A} \approx 2$ mW cm^{-1} K^{-1}. However, for the experimental data point at $x = 0.74$, there is a considerable difference from the calculated $S(-)$. This discrepancy we interpret in the following way.

For amorphous transition-metal–metalloid alloys, $\kappa_{e,i} = S_i^0 = 0$ for $\upsilon_i < 1/3$ is only an approximation, because, at the boundary faces between the different phases, there are p–d bonds, i.e. d orbitals of the Cr atoms (of the A phase grains) overlap with p orbitals of the boundary faces atoms on the B phase grains, resulting in a p–d band, which is incompletely occupied. (For a detailed discussion see section IIA of [8].) Because of this p–d overlapping, this (incompletely occupied) p–d band exists also if $\upsilon_A < 1/3$: although the energy levels of the s states in the separate A phase grains are discrete, the electrons can be activated to higher energies (at the hot end of the sample) and deliver energy (at the colder end) by a transition to the p–d band. That is why $\kappa_{e,A} \neq 0$ and $S_A^0 \neq 0$, also for $\upsilon_A < 1/3$. However, the real values of $\kappa_{e,A}$ and S_A^0 (for $\upsilon_A < 1/3$) are expected to be essentially smaller than as calculated by equations (21) and (20), because the d states are localized. On the other hand, for $\upsilon_B < 1/3$, the p–d band is not extended into the inside of the separate B phase grains. It is limited to the A phase and the boundary face atoms of the B grains, because the orbital configuration of the boundary face atoms (B^*) is different from those of the core atoms (B_0) (see figure 1 of [8]). That is why, also for $\upsilon_B < 1/3$, $\kappa_{e,B} \neq 0$ and $S_B^0 \neq 0$ must be assumed, although these values (for $\upsilon_B < 1/3$) are surely small compared with equations (21) and (20), because only the states of the boundary face atoms (B^*) are involved in the p–d band.

When non-zero values are assumed for $\kappa_{e,i}$ and S_i^0 (for $\upsilon_i < 1/3$), however, still small compared with the values calculated by equations (21) and (20), respectively, then the $S(-)$ curve approaches in direction to the experimental data point at $x = 0.74$, whereas on the metal-rich side ($\upsilon_B < 1/3$), the $S(-)$ curve is practically not changed. In figure 3, the dotted bold line is the $S(-)$ curve calculated for $\kappa_{ne,i} = 2$ mW cm^{-1} K^{-1} and $S_i^0 = \kappa_{e,i} = 0$ for $\upsilon_i < 1/3$ (indicated by 0%). The dotted–dashed line (indicated by 3%) is the $S(-)$ curve, where S_i^0 and $\kappa_{e,i}$ (for $\upsilon_i < 1/3$) are replaced by $0.03 \times S_A^0$ and $0.03 \times \kappa_{e,i}$ calculated by equations (20) and (21), respectively.

At the present time, we are not yet able to calculate precisely $\kappa_{e,i}$ and S_i^0 for $\upsilon_i < 1/3$. However, we believe that the calculated $S(-)$ curves in figure 3 reflect the general tendency of the concentration dependence of the thermopower at large x as well, i.e. a maximum is expected in the concentration range $0.67 < x < x_c$, where $x_c \approx 0.87$ is the concentration of the metal–insulator transition in a-Cr$_{1-x}$Si$_x$.

On the other hand, the good agreement between the calculated $S(-)$ and the experimental data for $x < 0.67$ suggests that the assumption of elastic scattering (assumption (a) , section 1) is actually fulfilled.

5.3. *Crystallization kinetics of amorphous metallic alloys*

The discussion in section 5.2 suggests that the Seebeck coefficient shows discontinuities at specific concentrations if the alloy is composed of different phases. This is a characteristic feature distinguishing composites from homogeneous alloys. By measurement of S versus x, these discontinuities can be determined experimentally. Thus x_A and x_B can be determined experimentally very precisely.

This result can be applied for characterization of the crystallization kinetics of amorphous transition-metal–metalloid alloys, easy to produce as thin films by co-sputtering or co-evaporation as described by Mangin *et al* [18] for a-Au$_{1-x}$Si$_x$. Mangin *et al* [18] have found that a-Au$_{1-x}$Si$_x$, in the Si-rich regime, is composed of two amorphous phases, a-Au$_{0.75}$Si$_{0.25}$ and a-Si, which we call phase A and phase B, respectively, i.e. $x_A = 0.25$ and $x_B = 1.00$. The phase A is identical with the a-μ phase used by Mangin *et al* [18]. With these x_A and x_B, it follows that the discontinuities at $\upsilon_B = 1/3$ and $\upsilon_A = 1/3$ are to be expected at $x_{\upsilon_B=1/3} = 0.47$ and $x_{\upsilon_A=1/3} = 0.73$, calculated by equation (22) with the atomic densities $\mathcal{N}_A = 5.8 \times 10^{22}$ cm^{-3} and $\mathcal{N}_B = 5.0 \times 10^{22}$ cm^{-3} taken from [18] (table I therein).

Considering the crystallization mechanism, in [18] it is supposed that, at increasing temperatures, the a-μ and a-Si phases crystallize separately into metastable c-μ and c-Si phases without long-range diffusion (diffusionless transformation) before reaching the equilibrium state characterized by a mixture of the crystalline phases c-Au and c-Si [30, 35]. Applying the result of section 5.2, this supposition by Mangin *et al* [18] can now be checked by measurement of S versus x at different temperatures. If this supposition is true, the discontinuities in S will be shifted to lower x after crystallization of a-$\mathrm{Au}_{1-x}\mathrm{Si}_x$; as long as the a-$\mu$ and a-Si phases transform diffusionless to c-μ and c-Si, the discontinuities are also expected at $x = 0.47$ and 0.73, if the atomic densities do not essentially change, while they are expected to be shifted to smaller x in the equilibrium state consisting of the phases c-Au and c-Si corresponding to $x_A = 0$ and $x_B = 1.00$. In this case, equation (22) provides $x_{\upsilon_B=1/3} = 0.30$ and $x_{\upsilon_A=1/3} = 0.63$ for the discontinuities, when additionally, $\mathcal{N}_A = 5.9 \times 10^{22}\ \mathrm{cm}^{-3}$, the atomic density of c-Au, is considered. This example, a-$\mathrm{Au}_{1-x}\mathrm{Si}_x$, shows that measurement of S versus x at different temperatures can provide additional information about the crystallization kinetics. Discontinuities are also expected in the concentration dependence of the heat conductivity. Measurement of κ at thin films is, however, more expensive and more difficult than measurement of S versus x.

6. Summary

The thermopower formula for composites derived in the present paper is

$$\sum_i \upsilon_i \frac{\kappa_i/S_i - \kappa/S}{\kappa_i/S_i + 2\kappa/S} = 0. \qquad (23)$$

While the thermopower formula derived in [1] is only an approximation formula for composites with metallic phases, equation (23) holds generally, also for composites containing metallic and/or semiconducting phases. A prerequisite for the applicability of equation (23) is the fact that each of the phases can be characterized by its own specific transport coefficients, κ_i and S_i, and that the phase grains are spherical without preferred orientations and arranged in a symmetrical fashion.

There are two contributions to S_i, a scattering term and a contribution due to electron transfer between the phases maintaining a common electrochemical potential.

In composites with metallic phases, S_i and κ_i change discontinuously at the transition from a macroscopic phase cluster to separate phase grains leading to discontinuities in the concentration dependence of the Seebeck coefficient. It is argued that in amorphous composites this transition occurs very precisely at $\upsilon_i = 1/3$. Discontinuities in the concentration dependence of S (and κ) is a characteristic feature for metallic alloys distinguishing composites from homogeneous alloys. It can be applied to characterize the crystallization kinetics of amorphous metallic composites. By experimental determination of these discontinuities, the average compositions of the phases can be determined.

Equation (23) and the theory described can be applied for calculating the Seebeck coefficient of amorphous transition-metal–metalloid alloys, because in this class of alloys amorphous phase separation is realized for large ranges of concentration. The theory is applied to a-$\mathrm{Cr}_{1-x}\mathrm{Si}_x$ alloys for calculating the Seebeck coefficient versus x. Both the calculated $S(x)$ dependence and the discontinuities agree very well with the experimental data, as long as $x < 0.67$; the deviations at $x > 0.67$ are interpreted to be caused by neglect of the p–d bonds at the phase boundaries. The good agreement between the calculated $S(-)$ and the experimental data for $x < 0.67$ supports the assumption of elastic scattering in the metallic regime of a-$\mathrm{Cr}_{1-x}\mathrm{Si}_x$ alloys.

Acknowledgments

I acknowledge Professor Dr Stolze from the University of Dortmund for proofreading the manuscript of this paper.

It is with great regret that I learnt about the premature death of Professor Dr Hellmut Keiter from the University of Dortmund. I want to use the opportunity to express my gratitude for his kind support in reading and correcting previous papers of mine.

References

[1] Sonntag J 2006 *Phys. Rev.* B **73** 045126
[2] Harman T C and Honig J M 1967 *Thermoelectric and Thermomagnetic Effects and Applications* (New York: McGraw-Hill)
[3] Barnard R D 1972 *Thermoelectricity in Metals and Alloys* (London: Taylor and Francis)
[4] Odelevskii V I 1951 *J. Tech. Phys. (USSR)* **21** 678
[5] Landauer R 1952 *J. Appl. Phys.* **23** 779
[6] Cohen M H and Jortner J 1973 *Phys. Rev. Lett.* **30** 696
[7] Kirejew P S 1978 *Semiconductor Physics* (Moscow: Mir)
[8] Sonntag J 2005 *Phys. Rev.* B **71** 115114
[9] Gladun C, Heinrich A, Lange F, Schumann J and Vinzelberg H 1985 *Thin Solid Films* **125** 101
[10] Weser A 1981 *PhD Thesis* Technische Universität Dresden
[11] Sonntag J 1980 unpublished
[12] Edwards A M, Fairbanks M C, Singh A, Newport R J and Gurman S J 1989 *Physica* B **158** 600
[13] Edwards A M, Fairbanks M C and Newport R J 1991 *Phil. Mag.* B **63** 457
[14] Regan M J, Rice M, Fernandez van Raap M B and Bienenstock A 1994 *Phys. Rev. Lett.* **73** 1118
[15] Lorentz R D, Bienenstock A and Morrison T I 1994 *Phys. Rev.* B **49** 3172
[16] Fernandez van Raap M B, Regan M J and Bienenstock A 1995 *J. Non-Cryst. Solids* **191** 155
[17] Regan M J and Bienenstock A 1995 *Phys. Rev.* B **51** 12170
[18] Mangin P, Marchal G, Mourey C and Janot C 1980 *Phys. Rev.* B **21** 3047
[19] Marchal G, Mangin P and Janot C 1980 *Phil. Mag.* B **423** 81
[20] Theye M L, Van V N and Fisson S 1983 *Phil. Mag.* B **47** 31
[21] Gurman S J, Williams B T and Amiss J C 2000 *J. Phys.: Condens. Matter* **12** 5981
[22] Williams B T, Gurman S J and Amiss J C 2000 *J. Phys.: Condens. Matter* **12** 5971
[23] Gärtner F, Michaelsen C and Bormann R 1997 *Phil. Mag.* B **76** 511
[24] Sonntag J 1989 *Phys. Rev.* B **40** 3661
[25] Goldsmid H J, Kaila M M and Paul G L 1983 *Phys. Status Solidi* a **76** K31
[26] Papa T, Scudieri F, Marinelli M, Zammit U and Cemhali G 1983 *J. Physique* **44** C5
[27] Wada H and Kamijoh T 1996 *Japan. J. Appl. Phys.* **35** L648
[28] Zink B L, Pietri R and Hellman F 2006 *Phys. Rev. Lett.* **96** 055902

[29] Graff K 1995 *Metal Impurities in Silicon-Device Fabrication* (Berlin: Springer)
[30] Shunk F A 1969 *Constitution of Binary Alloys* 2nd suppl. (New York: McGraw-Hill)
[31] Atkins P W and dePaula J 2006 *Physikalische Chemie* (Weinheim: Wiley–VCH)
[32] Atkins P W and dePaula J 2006 *Physical Chemistry 8/e* (Oxford: Oxford University Press)
[33] Samsonov G V, Dvorina L A and Rud B M 1979 *Silicides* (Moskau: Metallurgija)
[34] Kittel C 1971 *Festkörperphysik* (Leipzig: Akademische Verlagsgesellschaft)
[35] Hansen M and Anderko K 1958 *Constitution of Binary Alloys* (New York: McGraw-Hill)
[36] Airapetiants C V 1957 *Sov. Phys.—Tech. Phys.* **2** 429
[37] Webman I, Jortner J and Cohen M H 1977 *Phys. Rev.* B **16** 2959
[38] Halpern V 1983 *J. Phys. C: Solid State Phys.* **16** L217
[39] Xia T K and Zeng X C 1987 *J. Phys. C: Solid State Phys.* **20** L907
[40] Balagurov B Y 1986 *Sov. Phys.—Semicond.* **20** 805
[41] Bergman D J and Levy O 1991 *J. Appl. Phys.* **70** 6821
[42] Herring C 1960 *J. Appl. Phys.* **31** 1939
[43] Troadec J P and Bideau D 1981 *J. Physique* **42** 113
[44] Troadec J P and Bideau D 1983 *J. Phys. C: Solid State Phys.* **16** 1169
[45] Fishchuk I I 1990 *Sov. Phys.—Solid State* **32** 2053
[46] Ausloos M, Durczewski K, Patapis S K, Laurent C and Vanderschueren H W 1988 *Solid State Commun.* **65** 365
[47] Whall T E 1981 *J. Phys. C: Solid State Phys.* **14** L887
[48] Straley J P 1981 *J. Phys. D: Appl. Phys.* **14** 2101